Wettability of Fly Ashes from Four Coal-Fired Power Plants in China

ARTICLE *in* INDUSTRIAL & ENGINEERING CHEMISTRY RESEARCH · JUNE 2011

Impact Factor: 2.59 · DOI: 10.1021/ie2001378

5 AUTHORS, INCLUDING:

Hailong Li
Huazhong University of Science and Technol…
23 PUBLICATIONS **416** CITATIONS
SEE PROFILE

Junying Zhang
Huazhong University of Science and Technol…
57 PUBLICATIONS **895** CITATIONS
SEE PROFILE

Yongchun Zhao
Huazhong University of Science and Technol…
68 PUBLICATIONS **406** CITATIONS
SEE PROFILE

Chang-Yu Wu
University of Florida
158 PUBLICATIONS **2,547** CITATIONS
SEE PROFILE

I&EC research
Industrial & Engineering Chemistry Research

ARTICLE

pubs.acs.org/IECR

Wettability of Fly Ashes from Four Coal-Fired Power Plants in China

Hailong Li,[†] Junying Zhang,*[,†] Yongchun Zhao,[†] Chang-Yu Wu,[‡] and Chuguang Zheng[†]

[†]State Key Laboratory of Coal Combustion, Huazhong University of Science and Technology, Wuhan 430074, Hubei, China

[‡]Department of Environmental Engineering Sciences, University of Florida, Gainesville, Florida 32611, United States

ABSTRACT: Wet flue gas desulfurization, heterogeneous condensation, and chemical agglomeration have been reported to be promising methods for controlling fine particulate matter (PM) from coal combustion flue gas. The effectiveness of these processes is affected by the wettability of the fly ash particles. A novel method based on the flotation mechanism using a laser particle size analyzer was used to measure the wettability of fly ash particles in water, sodium dodecylbenzene sulfonate (SDBS), and Triton X-100 (TX100) solutions. Fly ash samples were collected from four coal-fired power plants in China [Xuanwei (XW), Jungar (JG), Xiaolongtan (XLT), and Yangzonghai (YZH)], representing high-silicon, high-aluminum, high-calcium, and high-iron fly ashes, respectively. The particle size distributions, surface areas, zeta (ζ) potentials, densities, chemical compositions, mineral compositions, and morphologies of the fly ash samples were investigated as well. $PM_{0.1}$ and PM_{10+} were readily wetted in water, but most particles within the 1−10-μm range exhibited lower wettabilities. The wettability of fly ashes in water is related to other physical or chemical characteristics and follows the trend YZH > XLT > XW > JG. For YZH fly ash, $PM_{0.1}$ and PM_1^+ can be completely wetted in water. For XW, JG, and XLT fly ashes, only $PM_{0.1}$ and PM_{10+} can be wetted completely in water. Addition of SDBS or TX100 promoted most wetting processes, and the promotional effect is also related to other characteristics of fly ash particles such as surface roughness, surface area, and ζ potential.

1. INTRODUCTION

Particulate matter (PM) is the major urban pollutant in most Chinese cities.[1] It has been reported that the average annual urban PM concentration of 113 major cities in China in 2009 was above 80 $\mu g \cdot m^{-3}$.[2] Coal combustion fly ashes not captured by air pollution control devices make a significant contribution to PM pollution, particularly the inhalable particles with mean diameters of less them 10 μm (PM_{10}).[3] Currently, PM emissions from Chinese coal-fired power plants are estimated to be 3.81 million tonnes per year or 44.6% of total PM emissions in China.[4] PM_{10} constitutes the majority of the PM emissions because most of the large fly ash particles in flue gas are effectively captured in existing air pollution control devices.[5] These small particles are present in high number concentrations, are often enriched with toxic species such as metallic species,[6,7] and have long residence times in the atmosphere. Hence, emission of PM_{10}, and especially $PM_{2.5}$ (particles less than 2.5 μm in diameter), from coal-fired power plants and its control have attracted great attention in China. However, with the rapid increase in energy demand in China, more coal is projected to be consumed in the near future, which will definitely result in more PM_{10} emissions from coal-fired power plants if there is no significant improvement in PM_{10} control strategies.

Although the existing PM control devices such as electrostatic precipitators (ESPs) and bag filters are very effective in removing PM from coal combustion flue gas, effective removal of inhalable PM_{10}, especially $PM_{2.5}$, from flue gas is still challenging. Several new technologies such as hybrid ESP/wet flue gas desulfurization (WFGD),[8,9] heterogeneous condensation,[10,11] acoustic agglomeration,[12] magnetic aggregation,[13,14] thermophoretic aggregation,[15] and chemical agglomeration[16,17] have been developed for the effective capture of fine particles. Among these new methods, WFGD, heterogeneous condensation, and chemical agglomeration utilize droplets to capture fine fly ash particles or enlarge their size. The droplet−particle collection is a balance between two competing effects: those of particle collision and attachment and those of detachment. Droplet−particle attachment and detachment are determined by the interfacial wetting properties. The probability that a captured particle does not detach from a droplet again is determined by its wettability,[18] and the effectiveness of contact between fly ash particles and droplets has also been reported to depend on the wettability of the fly ash particles.[19,20] Accordingly, the wettability of fly ash particles in aqueous solution determines the efficacy of these new methods for the removal of PM_{10} from coal combustion flue gas. However, to the best of our knowledge, only a few studies on the wettability of fly ash have been conducted. Yan et al.[19] measured the wettability of fly ash from both coal combustion and solid waste incineration using a capillary pressure method. In that research, a Washburn tube closed by a filter at the bottom was filled with 3−4 g of fly ash particles. The bottom of the tube was brought into contact with liquid, which could rise into the tube through the capillary effect of the voids between the particles. The contact angle, which represents the wettability of the particles, was calculated from the pressure variation during the rise of the liquid. This capillary rise method relies on the assumption that a powder can be treated as a bundle of capillaries and depends on the specific model applied.[18] In addition, experimental errors would be brought into the system during the process of filling the Washburn tube with particles. Furthermore, it takes great effort to get several grams of fine particles, especially submicrometer particles, to

Received: January 19, 2011
Accepted: May 16, 2011
Revised: April 28, 2011
Published: May 16, 2011

dx.doi.org/10.1021/ie2001378 | *Ind. Eng. Chem. Res.* 2011, 50, 7763–7771

meet the needs of this capillary pressure method. In addition to contact angle measurements, the flotation approach is also commonly used for identifying the wettability of solid particles.[21] The principle of flotation is that hydrophilic particles settle to the container bottom because the gravity of the particles is larger than the buoyancy force, but hydrophobic particles allow bubbles to attach to them and suspend in solution or float on the solution surface. The efficiency of flotation is known to decrease with increasing particle wettability.[22,23] Obviously, the wettability of solid particles can be described by the efficiency of flotation or the reverse sedimentation. Therefore, by measuring the variation in the particle size distribution (PSD) due to sedimentation, the wettability of the particles can be determined.[24]

In this work, the wettability of Chinese fly ashes from four power plants was tested using a novel method based on the variation of the PSD before and after wetting/sedimentation. The main advantages of this method are its requirement for only a small quantity of sample and its high reproducibility through precise control of experimental conditions. Other physical and chemical characteristics of these fly ashes were studied as well because both their chemical properties (composition) and their physical properties (surface area, roughness, shape, and particle size) influence their wettability.[25] The objective of this study was to identify the wettability characteristics of different coal combustion fly ashes and analyze the possible relationships between wettability and other physical and chemical properties. The findings of this research will provide fundamental information for the development of effective PM_{10} control technologies for coal-fired power plants.

2. FLY ASH SAMPLES AND EXPERIMENTAL METHODS

2.1. Fly Ash Samples and Wetting Agents. Fly ash samples were collected from the hoppers of ESPs at four coal-fired power plants in Xuanwei (XW), Jungar (JG), Xiaolongtan (XLT), and Yangzonghai (YZH) in China. These fly ash samples were sieved through a 500-mesh sieve to less than 25 μm for investigation, because larger fly ash particles were found to be wetted easily in our previous study.[26]

Usually, anionic and nonionic surfactants can be used as wetting agents. In this research, sodium dodecyl benzene sulfonate (SDBS) and Triton X-100 (TX100) were used as anionic and nonionic wetting agents, respectively. The surface tension of wetting agents was determined by the drop-weight measurement technique using a surface tension instrument (model K99B, Powereach, Inc.). As shown in Figure 1, SDBS and TX100 lowered the surface tension of water from 72.75 to less than 40 $mN \cdot m^{-1}$ at room temperature. The surface tension of water decreased swiftly upon addition of TX100.[27] Introduction of 0.05% TX100 into water resulted in a surface tension of 33.0 $mN \cdot m^{-1}$, which is almost the same as that of 0.2% SDBS solution.

2.2. Characterization of Fly Ashes. A Master Min laser particle size analyzer (model MNM 5004, Malvern Instruments Ltd.) with a detection range from 0.05 to 900 μm was used to measure the PSDs of original fly ash samples (less than 25 μm). Particulate samples were dispersed in water by a mechanical stirrer at low speed and ultrasound with a relative intensity of 60 (on an instrumental range from 0 to 100) for 2 min before size measurement. Brunauer−Emmett−Teller (BET) surface area analysis by N_2 adsorption was performed using an ASAP 2020 micropore analyzer from Micromeritics. Fly ash samples were

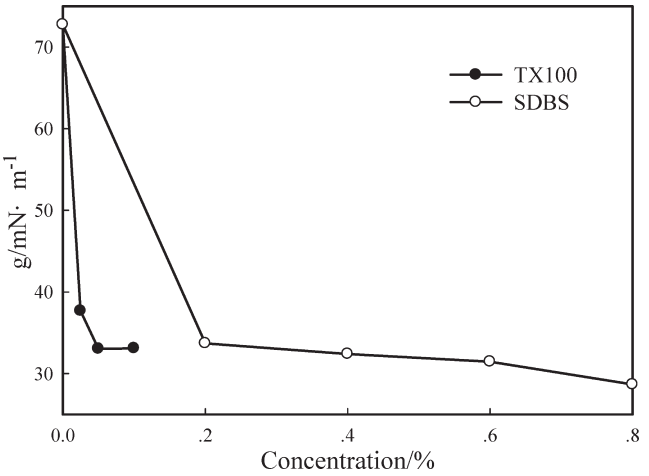

Figure 1. Surface tensions of wetting agents at 20 °C.

dispersed in nanopure water for zeta (ζ) potential analysis using a Zetasizer Nano Instrument (model ZC-2000, Macrotech Nichion). Density measurements were carried out using a commercial helium pycnometer (model 1330, Micromeritics Inc.). X-ray fluorescence (XRF) spectrometry was used to determine the oxides of major elements, including SiO_2, Al_2O_3, CaO, Fe_2O_3, K_2O, Na_2O, MgO, and SO_3. The minerals in fly ash samples were identified by X-ray diffraction (XRD) using an X′Pert PRO diffractometer equipped with a graphite diffracted-beam monochromator. The XRD patterns were recorded over a 2θ interval of 10−70°, with a step size of 0.017° and a counting time of 10 s per step. The morphological properties of fly ash samples were investigated by field-emission scanning electron microscopy (FESEM) using a Sirion200 microscope equipped with a GENESIS EDX (energy-dispersive X-ray spectroscopy) attachment.

2.3. Wettability Tests. In these tests, 0.2-g fly ash samples were first dispersed in 100 mL water or wetting agent solutions (0.2% SDBS or 0.05% TX100) to form slurries in which the fly ash particles were wetted under ultrasonic exposure for 5 min. The ultrasound was employed to promote the dispersion of the fly ash particles. In addition, ultrasonic waves consist of compression and rarefraction cycles that could produce cavitation bubbles in the slurries.[28] These bubbles might attach to hydrophobic particles and make them float in the solution rather than settle to the bottom of the container. After the wetting process, the slurries were allowed to settle for 3 min. Then, 75 mL of solution from the upper part of the container was collected for further PSD measurement. Before PSD measurements, the 75 mL of solution obtained from the wetting/sedimentation process were dispersed using the same procedure as for the dispersion of particulate samples described above. According to the flotation mechanism, wetted particles settle to the bottom of the container, whereas nonwetted particles float in solution. The variation of the PSD in solution was due to the wetting of particles. By comparing the difference in PSDs before and after the wetting/sedimentation process, the wettability of fly ashes and even the wettability of particles in a specific diameter range can be obtained. Five replicates were obtained for each experimental condition, and the mean value after subtraction of the background particle concentration of water or wetting agents was reported. All wetting experiments were conducted at room temperature (20−25 °C). It should be noted that the flue gas

temperature is much higher than room temperature. The effect of temperature on the wettability of fly ash was studied in our previous research where better wetting performance was found to be at higher temperature, especially in wetting agent solutions.[20]

3. RESULTS AND DISCUSSION

3.1. Particle Size Distribution. The PSD is one of the most important physical characteristics of PM. The number-based PSD curves of fly ash samples are shown in Figure 2. As shown, bimodal size distributions with one peak in the PM_{10+} (particles larger than 10 μm in diameter) range and the other peak in the $PM_{0.1}$ (particles smaller than 0.1 μm in diameter) range were observed for JG, XLT, and YZH samples, whereas XW fly ash exhibited a bimodal size distribution with a large peak in the PM_{10+} range and the other minor peak around 0.3 μm. Most particles in these samples were $PM_{2.5+}$ (particles larger than 2.5 μm in diameter) or $PM_{0.1}$. Very few particles were in the 0.1−1 μm range. Although these fly ash samples were sieved through a 500-mesh sieve, the results still indicate that the removal efficiency of ESP for particles with diameters between 0.1 and 1 μm is low. This is in line with other study results that the penetration of submicrometer particles was 30 times the overall penetration in a full-scale ESP.[29] The reason is that both diffusion charging and field charging responsible for particle removal in ESP are not effective for particles between 0.1 and 1 μm.

The characteristic diameters including the mean diameter (D_{50}) and boundary diameters (D_{10}, D_{90}) were used to express the PSD of each sample. The numbers (i.e., 50, 10, 90) in D_{50}, D_{10}, and D_{90} stand for the percentages of the total number of particles below the specified diameters. As shown in Table 1, the mean diameters of all of the original samples were around 10 μm.

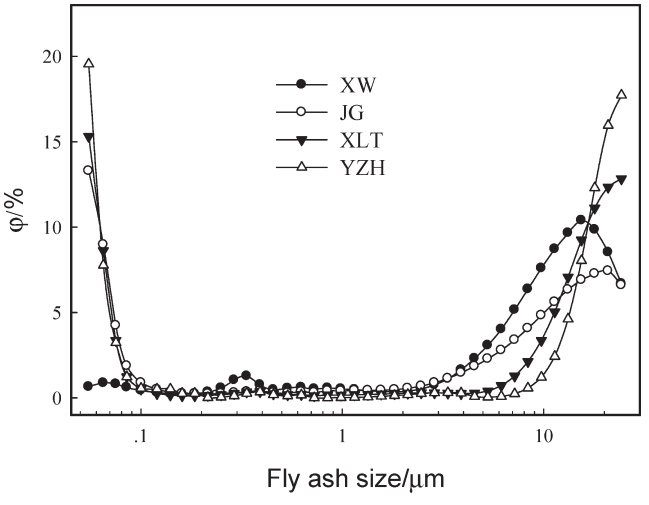

Figure 2. Particle size distribution of fly ash samples.

3.2. Surface Area, ζ Potential, and Density. Interfacial reaction including wetting can be enhanced by the greater specific surface area associated with rough surfaces.[30] The vast majority of coal fly ash particles are nonporous, and their surface area is almost entirely due to the external surface.[31] Therefore, fly ash particles with higher external roughness generally have higher surface areas. As shown in Table 2, YZH fly ash had the highest surface area, whereas JG fly ash had the lowest surface area. The surface areas of all fly ash samples were almost lower than 1 $m^2 \cdot g^{-1}$, which is much lower than that of other coal fly ashes[32,33] because unburned carbon with large surface area usually exists in large particles and was sieved out of the samples. The ζ potential results show that all fly ash samples carried negative charges. JG fly ash had the lowest ζ potential of −33.4 mV, indicating there were more negative charges on its surface. The true density of each fly ash sample was larger than 2.5 $g \cdot cm^{-3}$, which is much higher than that of water. Therefore, fly ash particles should settle swiftly to the bottom of the container if they are completely wetted. No obvious difference in density was observed among these four fly ash samples. Hence, the sedimentation error caused by particle density was negligible.

3.3. Chemical Composition. The chemical compositions of fly ash samples and the average chemical composition[34] of Chinese fly ashes are listed in Table 3. The primary chemical components of these four fly ashes were similar to those of other fly ashes,[35] including SiO_2, Al_2O_3, CaO, and Fe_2O_3. The content of SiO_2 in XW fly ash was 61.78%, which is higher than the average SiO_2 content of Chinese fly ashes. This was probably due to the unique characteristics of XW coal, in which the silicon and free silica concentrations were reported to be 10 times higher than those of other coals.[36] JG fly ash was highly enriched in Al_2O_3 (50.57%) because the feed coals were rich in aluminum-bearing minerals.[37] Usually, combustion of low-rank lignite coals generates high-calcium fly ashes (with CaO content of 15−30%).[38] XLT high-calcium fly ash with a CaO content of 29.34% was from the combustion of XLT lignite. For YZH fly ash, the Fe_2O_3 content was 12.82%, which is almost twice the average value of Chinese fly ashes. Pyrite in the feed coals of the YZH power plant was responsible for the high Fe_2O_3 content.[39] According to standard ASTM C618,[40] fly ashes containing more

Table 2. BET Surface Areas, ζ Potentials, and Densities of Fly Ash Samples

fly ash	BET surface ($m^2 \cdot g^{-1}$)	ζ potential (mV)	true density ($g \cdot cm^{-3}$)
XW	0.79	−23.5	2.51
JG	0.65	−33.4	2.52
XLT	0.96	−12.4	2.66
YZH	1.06	−26.1	2.78

Table 1. Characteristic Diameters (μm) of Four Fly Ash Samples under Different Conditions

	XW			JG			XLT			YZH		
conditions	D_{10}	D_{50}	D_{90}	D_{10}	D_{50}	D_{90}	D_{10}	D_{50}	D_{90}	D_{10}	D_{50}	D_{90}
original sample	0.62	10.40	23.02	0.06	6.89	22.77	0.06	12.03	21.66	0.06	14.30	22.40
water	0.35	5.60	11.34	0.92	5.97	13.88	0.25	2.28	7.17	0.08	0.17	0.98
0.2% SDBS	0.23	3.52	8.06	0.86	5.70	16.41	0.16	0.62	4.53	0.09	0.34	2.66
0.05% TX100	0.54	2.32	5.26	0.73	5.29	15.40	0.84	0.25	7.18	0	0	0

dx.doi.org/10.1021/ie2001378 |Ind. Eng. Chem. Res. 2011, 50, 7763–7771

Table 3. Major Chemical Composition of Fly Ash Samples (wt %)

fly ash	SiO_2	Al_2O_3	Fe_2O_3	CaO	MgO	K_2O	Na_2O	SO_3
XW	61.78	23.11	7.37	2.27	1.36	0.86	0.44	0.19
JG	41.32	50.57	2.15	2.43	0.63	0.46	1.25	0.36
XLT	30.87	15.48	11.33	29.34	2.05	0.91	1.49	3.42
YZH	45.00	25.29	12.82	7.62	4.02	1.67	0.65	1.32
mean value for Chinese fly ashes[34]	50.6	27.2	7.0	2.8	1.2	1.3	0.5	0.3

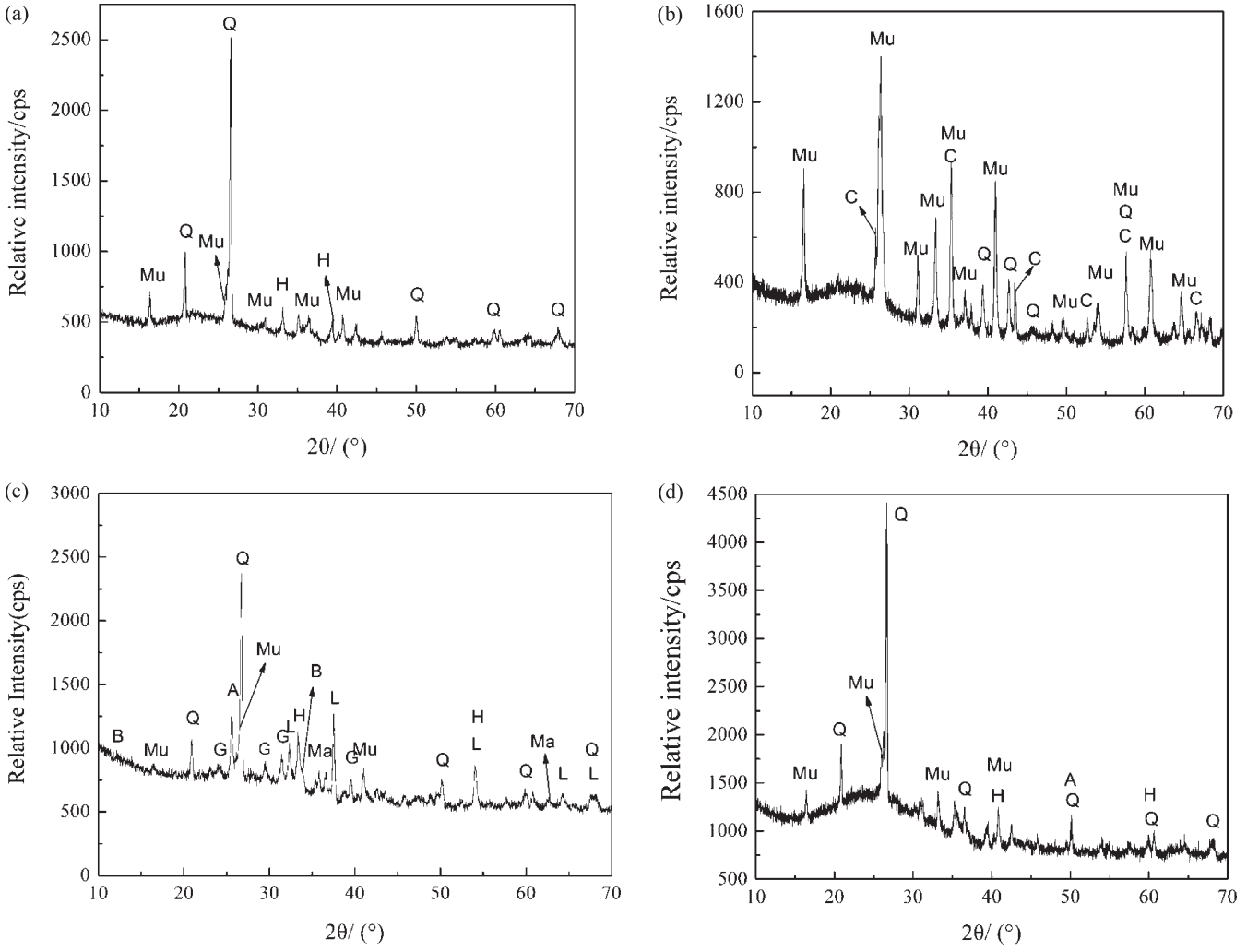

Figure 3. X-ray diffraction patterns of fly ash samples: (a) XW, (b) JG, (c) XLT, and (d) YZH fly ash. Mineral abbreviations: A = anhydrite, B = brownmillerite, C = corundum, G = gehlenite, H = hematite, L = lime, Ma = magnetite, Mu = mullite, Q = quartz.

than 70% $SiO_2 + Al_2O_3 + Fe_2O_3$ and low levels of CaO are defined as class F, whereas those with $SiO_2 + Al_2O_3 + Fe_2O_3$ contents between 50% and 70% and high CaO contents are defined as class C. XW and JG fly ashes are typical class F fly ashes, whereas XLT fly ash belongs to class C. YZH fly ash also belongs to class F, but its calcium content is much higher than those of XW and JG fly ashes.

3.4. Mineralogical Properties. Flotation is widely used to quickly and efficiently separate valuable minerals from other minerals, because different minerals have different wettability characteristics.[41] The mineralogical composition of fly ash can affect its wettability. XRD patterns of the investigated fly ash samples are presented in Figure 3, and the species were identified by comparing XRD patterns with International Centre for Diffraction Data (ICDD) files. As shown, in every sample, quartz (SiO_2) and mullite ($Al_6Si_2O_{13}$) were identified. The background hump between 10° and 40° in the XRD spectra evidences the presence of amorphous-phase aluminosilicate glass, which was generated as a result of rapid cooling at high temperature. Aluminosilicate glass, mullite, and quartz are always present as the major phases in coal combustion fly ash.[33] Among them, mullite in coal combustion fly ash is due to the thermal decomposition of kaolinite,[42] which is a major mineral phase in most coals.

dx.doi.org/10.1021/ie2001378 |*Ind. Eng. Chem. Res.* 2011, 50, 7763–7771

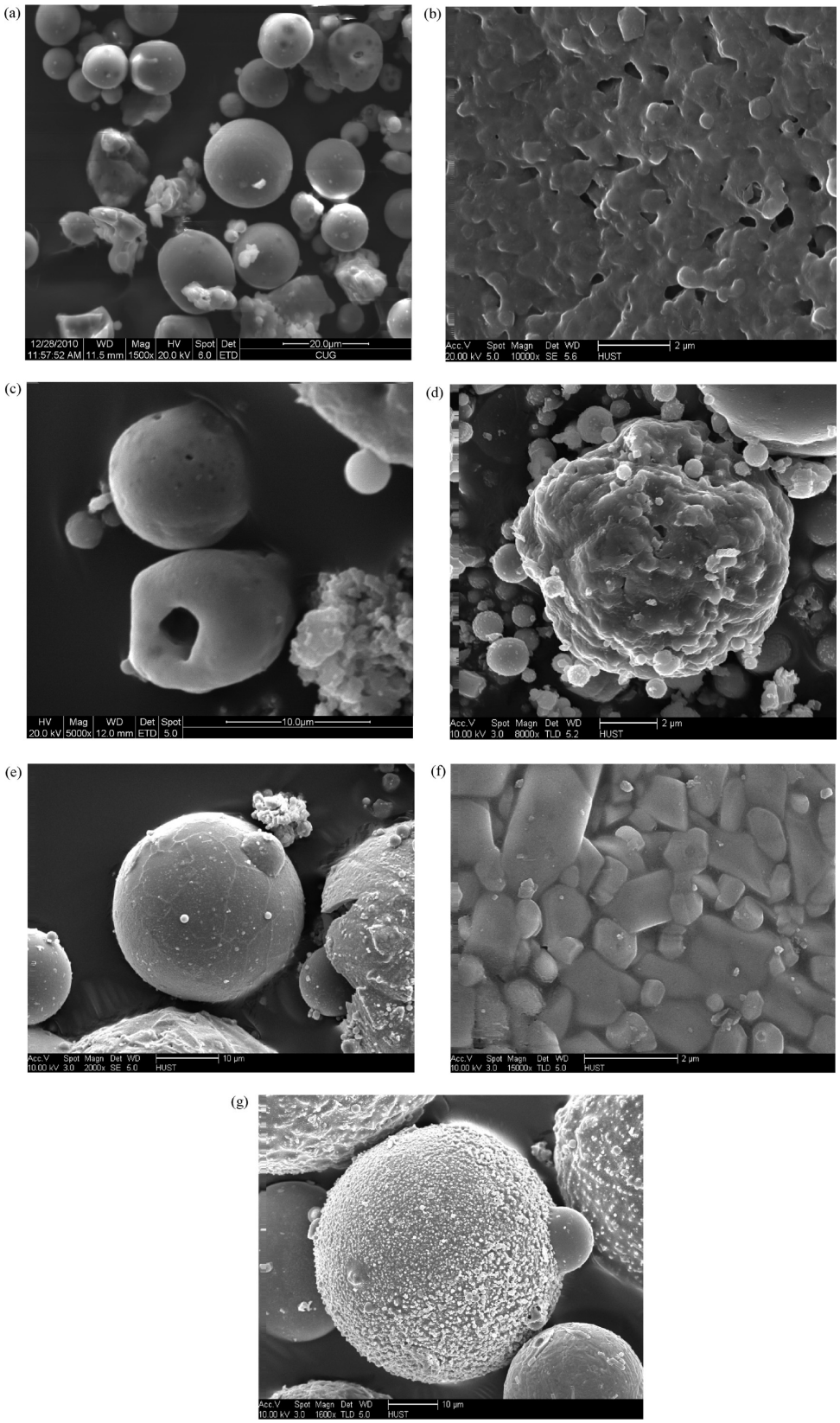

Figure 4. SEM images of fly ash samples: (a) XW fly ash particles, (b) agglomerate of fine particles in JG fly ash, (c) coarse particles in JG fly ash, (d) fine particles in XLT fly ash, (e) coarse particles in XLT fly ash, (f) fine particles in YZH fly ash, and (g) coarse particles in YZH fly ash.

For XW fly ash with a high silicon content, the most abundant mineral was quartz; mullite and hematite were also observed. This is in accordance with another study where the dominant mineral in XW coals was found to be quartz.[36] The Si/Al weight ratio of XW fly ash was 2.67, which is much higher than those of other fly ashes. This high Si/Al ratio also suggests the presence of free silica in XW fly ash, because the average Si/Al ratio of aluminosilicate is about 1.5.[43] The vaporization−condensation mechanism is not responsible for quartz formation during coal combustion because quartz is one of the least reactive minerals in coal.[43] Rather, the fragmentation of the quartz in coal is likely the source of the quartz in XW fly ash. It should be noted that quartz is a highly hydrophilic solid that interacts strongly with water molecules on its surface.[44]

For JG fly ash with a high aluminum content, the minerals identified by XRD included mullite, corundum, and quartz. The high mullite content of JG fly ash was due to the high kaolinite content of the feed coals at the JG power plant.[37] Corundum is generally rare in coal fly ash, although it has been observed in some coals[45] and high-temperature ashes[46] as an accessory minor mineral. Corundum was observed in JG fly ash, whereas no corundum was identified in the feed coals. Transformation of boehmite in the feed coals during coal combustion was the reason.[37] Only a few weak quartz peaks were observed in the XRD pattern, indicating a low content of quartz in JG fly ash. This is in line with another study where the quartz in JG fly ash was found to be less than 2%.[37] Most of the silicon in JG fly ash existed as an amorphous glass phase.

For XLT fly ash with a high calcium content, aside from mullite and quartz, the main calcium-bearing minerals included oxides, sulfates, and aluminosilicates, as shown in Figure 3c. Calcium oxide is the characteristic phase of the coal combustion product. Sulfate was probably derived from the dehydration of gypsum in XLT coal. Calcium aluminosilicates are the most common calcium-bearing minerals in fly ash and are derived from the reaction between aluminosilicates and carbonate-bonded calcium, which is the dominant calcium species in XLT coal.[47]

For YZH fly ash with a high iron content, the most abundant iron-bearing mineral was hematite. The occurrence of hematite in YZH fly ash was due to the oxidation of ferric sulfides, sulfates, carbonates, and magnetite, as well as some dehydroxylation of goethite and lepidocrocite.[48] The contact angle of pure hematite from both natural and synthetic origins has been reported to range from 15° to 46°, demonstrating that hematite is hydrophilic.[49]

3.5. Morphology. Most particles in these four fly ash samples were observed to be well-rounded and spherical in shape. This is in line with other reports that fly ash particles from pulverized coal combustion are primarily spherical.[1,31] Only a few particles were irregular in shape. FESEM imagines of the fly ash samples are shown in Figure 4. As shown in Figure 4a, most XW fly ash particles were spheres or approximate spheres with diameters larger than 2.5 μm. Few $PM_{2.5}$ particles were observed to be irregular. In line with the PSD curves shown in Figure 2, almost no $PM_{0.1}$ was observed in XW fly ash. Agglomerates consisting of many nanoscale particles can be seen in Figure 4b, indicating the formation of nanoscale particles during the combustion of JG coal. This is in accordance with Figure 2, which shows a prominent peak for $PM_{0.1}$ in the PSD curve of JG fly ash. Most of these fine particles were reported to be irregular Al_2O_3 crystal particles that were due to the transformation of boehmite during coal combustion.[39] Coarse particles in JG fly ash (Figure 4c) existed as spheres or approximate spheres with extremely smooth surfaces. For XLT fly ash, fine particles (Figure 4d) were irregular in shape and rough on the surface or had smaller particles attached. Coarse particles (Figure 4e) were spheres, with plenty of wrinkles and few smaller attached particles on the surface. Fine particles in YZH fly ash (Figure 4f) were granular crystals with edges and corners. These fine granular crystals with different structures varied from nanoscale to microscale. Ferroaluminosilicates and ferrooxides such as hematite were the primary mineral phases of these fine particles according to EDX and XRD analysis. Coarse YZH fly ash particles (Figure 4g) were observed to be spheres with rough surfaces. For most cases, the external surfaces of these large spheres had plenty of fine particles attached, which greatly enhanced the surface roughness of the coarse particles.

3.6. Wettability. The PSD curves of original fly ash samples and particles in 75 mL of solution are shown in Figure 5. The characteristic diameters obtained from the PSD curves are summarized in Table 1. For all fly ash samples, the peak within the PM_{10+} range on the PSD curves moved to the PM_{10} range after the wetting/sedimentation process, indicating that PM_{10+} can be wetted more easily than PM_{10}. For JG, XLT, and YZH fly ashes, the amount of $PM_{0.1}$ decreased abruptly after wetting/sedimentation, implying good wettability of these fine particles, which were observed to have irregular shapes or rough surfaces. This is in accordance with another research indicating that particles with high surface roughness have high hydrophilicity.[21] In the slurry, the relative proportion of particles with a specific size range increased as other particles were wetted and settled to the bottom. For particles within the diameter range of 0.1−2.5 μm, their relative proportion increased (except in YZH fly ash in TX100 solution) after the wetting/sedimentation process because the wetting rate of particles in this size range was lower than that of other particles.

As shown in Figure 5a, after wetting/sedimentation, the larger peak in the PSD curve of XW fly ash moved to the PM_{10} range, and the smaller peak in the submicrometer range became more obvious. Wetting/sedimentation in water resulted in a decrease of D_{50} from 10.40 to 5.60 μm, indicating that larger particles were wetted in water. Introduction of 0.2% SDBS or 0.05% TX100 into water further decreased D_{50} from 5.60 to 3.52 or 2.32 μm, respectively. The lower surface tensions of the SDBS and TX100 solutions were responsible for the enhancements of the wetting performance. It should be noted that the surface tensions of the TX100 and SDBS solutions used in this study were almost the same. However, the TX100 solution exhibited better performance. As stated above, fly ash particles carry negative charges on their surface. Hence, a nonionic surfactant such as TX100 has a stronger affinity with fly ash particles than does an ionic surfactant such as SDBS. The upper boundary of the particle diameters in water was around 10 μm, indicating almost all PM_{10+} was wetted in water. The enrichment of quartz in XW fly ash was at least partly responsible for its good wettability. With the addition of SDBS or TX100, only a small fraction of $PM_{2.5+}$ was wetted. The wetting agents exhibited insignificant enhancement of the wetting performance because only limited wetting agents could be adsorbed on XW fly ash particles with low surface area and low roughness.

For JG fly ash, coarse particles were difficult to wet with water or wetting agents, as demonstrated by the minor shift in the PSD curves in Figure 5b. Wetting/sedimentation in water resulted in only a slight decrease of D_{50} from 6.89 to 5.97 μm. Roughness is the most striking property of solid surfaces, and particles with

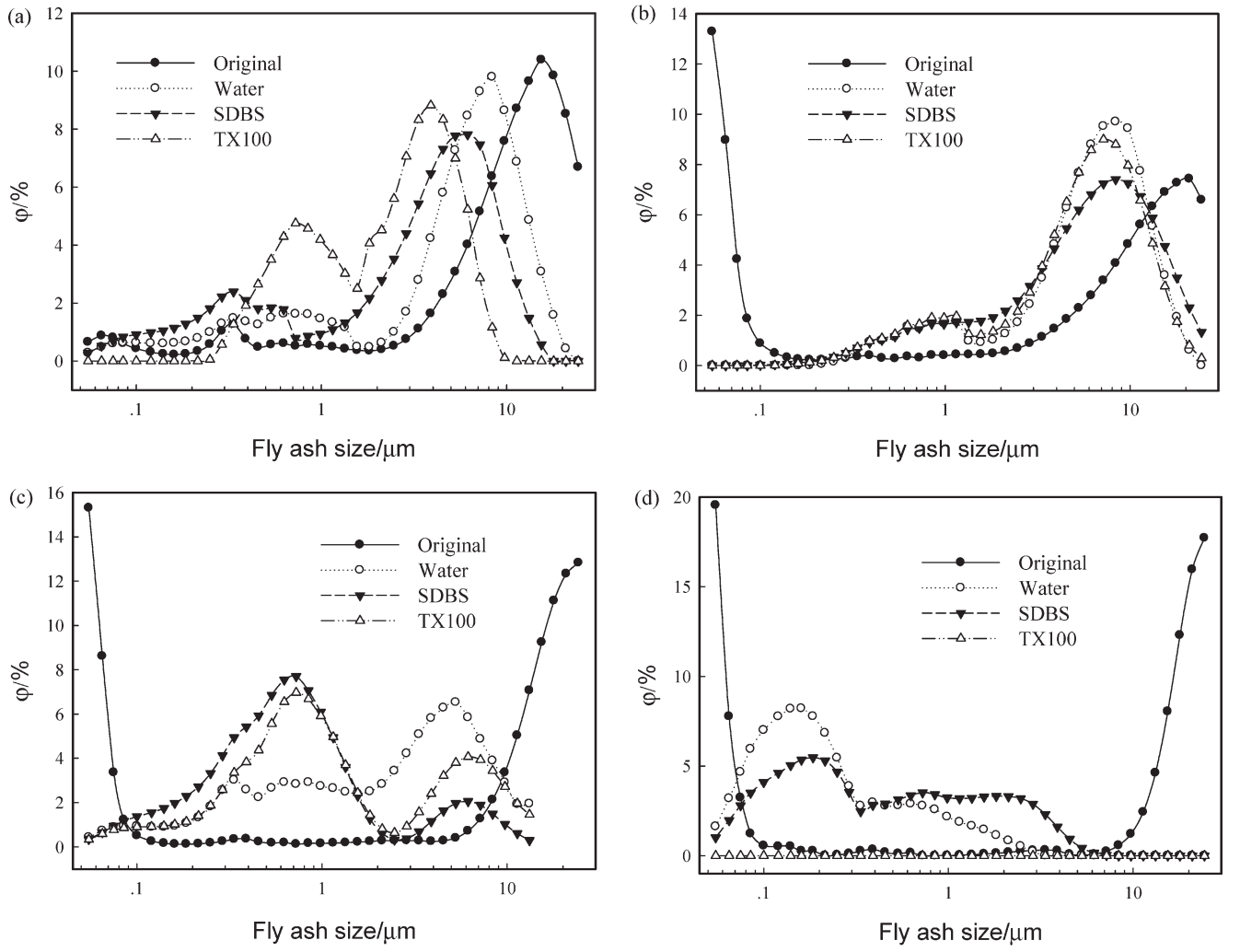

Figure 5. Particle size distributions of different fly ashes before and after wetting/sedimentation: (a) XW, (b) JG, (c) XLT, and (d) YZH fly ash.

lower surface roughness values have been reported to have higher hydrophobicities.[21] A smooth surface with a low surface area and low roughness was one important reason for the low wettability of JG fly ash. Moreover, the low content of hydrophilic quartz in JG fly ash might be another reason for its poor wetting behavior in water. Addition of SDBS or TX100 resulted in no obvious enhancement of the wetting performance, because it was hard for surfactant molecules to adsorb on JG fly ash particles with smooth surfaces and low surface areas. It should be noted that JG fly ash had the lowest ζ potential among the four studied fly ashes. Highly negative charges on JG fly ash particles inhibited the adsorption of surfactants, especially the anionic surfactant SDBS.

After wetting/sedimentation, two peaks in the $PM_{0.1}$ and PM_{10^+} ranges in the PSD curve of original XLT fly ash disappeared. Instead, two new peaks emerged in the PSD curves in the 0.1−2.5- and 2.5−10-μm ranges (Figure 5c). PM_{10^+} had better wettability than PM_{10}. Slower wetting and subsequent sedimentation of PM_{10} resulted in the increase of its relative proportion. The peaks in the 0.1−2.5-μm range were also due to the lower wetting rate of particles in this size range. As a result of the water wetting, D_{50} decreased from 12.03 to 2.28 μm. This large change in D_{50} indicates a high wettability of XLT fly ash in water. Two factors are responsible for this high wettability of XLT fly ash in water: (1) Physically, most XLT fly ash particles had rough surfaces and exhibited relatively higher surface areas than XW and JG fly ashes. (2) Chemically, XLT fly ash was rich in calcium-bearing minerals such as lime and anhydrite, which have intense interactions with water (i.e., lime adsorbs water to form calcium hydroxide, and anhydrite adsorbs water to form gypsum). D_{50} further decreased to 0.62 and 0.25 μm when SDBS and TX100, respectively, were added, demonstrating that the addition of SDBS and TX100 enhanced the wetting performance of XLT fly ash. The enhancement in wetting performance was at least partially due to the low surface tensions of the SDBS and TX100 solutions. Generally, repulsive forces between particles and surfactant molecules are smaller when the particles have higher ζ potentials. Comparing of the promoting effects of SDBS and TX100 on wetting performance among all fly ashes, the highest ζ potential of XLT fly ash was responsible for the best promoting effects of the wetting agents.

After wetting/sedimentation in both water and the wetting agents, $PM_{0.1}$ and PM_{10^+} of YZH fly ash almost disappeared. D_{50} decreased from 14.30 to 0.17, 0.34, and 0 μm, respectively, after wetting/sedimentation in water and SDBS and TX100 solutions, respectively. YZH fly ash had good wettability in water and the wetting agents, indicating that there were abundant hydrophilic

dx.doi.org/10.1021/ie2001378 |*Ind. Eng. Chem. Res.* 2011, 50, 7763–7771

lattices on its surface. In YZH fly ash, the abundant elements Si and Fe partially existed as quartz and hematite, which are hydrophilic. YZH fly ash had a relatively large surface area and high roughness degree, both of which facilitate wetting of particles. These factors in combination resulted in the excellent wettability of YZH fly ash. In SDBS solution, the characteristic diameters were slightly higher than in pure water, implying that the addition of SDBS inhibited the wetting process even though the surface tension of the SDBS solution was lower than that of water. YZH fly ash particles were rich in hydrophilic lattices, and part of hydrophilic lattices might be covered by the hydrophobic side of SDBS molecules. Therefore, the wettability of YZH fly ash decreased slightly upon the addition of SDBS.

4. CONCLUSIONS

The wettability of fly ash in water depends on various physical and chemical characteristics of fly ash particles such as size, shape, surface area, ζ potential, chemical composition, and mineral composition. $PM_{0.1}$ and PM_{10+} are readily wetted in water, whereas most PM_{10} has lower wettability. The wettabilities of the four studied fly ashes in water was found to follow the trend YZH > XLT > XW > JG. For YZH fly ash, $PM_{0.1}$ and PM_1^+ can be completely wetted in water. For XW, JG, and XLT fly ashes, only $PM_{0.1}$ and PM_{10+} can be wetted completely in water. The addition of wetting agents promoted the wetting process because they lowered the surface tension of water and changed the hydrophilic characteristics of the particle surface. In the wetting agents, the wettabilities of the fly ashes were still related to other physical and chemical characteristics. For JG fly ash with a low surface roughness, low surface area, and low ζ potential, an insignificant promoting effect of the wetting agents was observed. In contrast, a significant promoting effect of the wetting agents was observed for XLT fly ash with a high surface roughness, high surface area, and high ζ potential.

This study provides a new method for measuring the wettability of fly ash particles. The wettabilities of different fly ashes from Chinese coal-fired power plants were identified using this method. In addition, the relationships between wettability and other physical and chemical characteristics were studied. Such knowledge is of fundamental importance in developing effective water-based PM_{10} emission control technologies for coal-fired power plants.

AUTHOR INFORMATION

Corresponding Author

*E-mail: jyzhang@hust.edu.cn.

ACKNOWLEDGMENT

This project was supported by the National Natural Science Foundation of China (NSFC) (Nos. 40972102, 50906031, and 50936001) and the National Key Basic Research and Development Program (973) (No. 2010CB227003). The authors acknowledge Mr. Yan Yang and Mrs. Lin Huang for their assistance with the wetting experiments. Also, they thank the technicians from Analytical and Testing Center in Huazhong University of Science and Technology for helping with the chemical, mineral and morphological analyses.

REFERENCES

(1) Yao, Q.; Li, S. Q.; Xu, H. W.; Zhuo, J. K.; Song, Q. Studies on formation and control of combustion particulate matter in China: A review. *Energy* **2009**, *34* (9), 1296–1309.

(2) *2009 Report on the State of the Environment in China*; State Environmental Protection Administration: Beijing, 2010.

(3) Chen, Y. Z.; Shah, N.; Huggins, F. E.; Huffman, G. P.; Linak, W. P.; Miller, C. A. Investigation of primary fine particulate matter from coal combustion by computer-controlled scanning electron microscopy. *Fuel Process. Technol.* **2004**, *85* (6−7), 743–761.

(4) National Bureau of Statistics of China. *China Statistical Yearbook*; China Statistics Press: Beijing, 2006.

(5) Zhuang, Y.; Biswas, P. Submicrometer particle formation and control in a bench-scale pulverized coal combustor. *Energy Fuels* **2001**, *15* (3), 510–516.

(6) Pratim, B.; Wu., C. Y. Control of toxic metal emissions from combustors using sorbents: A review. *J. Air Waste Manage. Assoc.* **1998**, *48* (2), 113–127.

(7) Kersch, C.; Woerlee, G. F.; Witkamp, G. J. Supercritical fluid extraction of heavy metals from fly ash. *Ind. Eng. Chem. Res.* **2004**, *43* (1), 190–196.

(8) Meij, R.; Winkel, H. T. The emissions and environmental impact of PM_{10} and trace elements from a modern coal-fired power plant equipped with ESP and wet FGD. *Fuel Process. Technol.* **2004**, *85* (6−7), 641–656.

(9) Wang, H; Li, S. Q.; Yao, Q; Chen, C. H. Experimental study on removal effect of wet flue gas desulfurization system on fine particles from a coal-fired power plant. *Proc. Chin. Soc. Electr. Eng. (China)* **2008**, *28* (5), 1–6.

(10) Yang, L. J.; Bao, J. J.; Yan, J. P.; Liu, J. H.; Song, S. J.; Fan, F. X. Removal of fine particles in wet flue gas desulfurization system by heterogeneous condensation. *Chem. Eng. J.* **2010**, *156* (1), 25–32.

(11) Yan, J. P.; Yang, L. J.; Zhang, X.; Sun, L. J.; Zhang, Y.; Shen, X. L. Separation of $PM_{2.5}$ from combustion based on vapor condensation and scrubbing. *J. Fuel Chem. Technol. (China)* **2008**, *36* (3), 267–272.

(12) Sheng, C. D.; Shen, X. L. Simulation of acoustic agglomeration processes of poly-disperse solid particles. *Aerosol Sci. Technol.* **2007**, *41* (1), 1–13.

(13) Kumar, P.; Biswas, P. Analytical expressions of the collision frequency function for aggregation of magnetic particles. *J. Aerosol Sci.* **2005**, *36* (4), 455–469.

(14) Li, Y. W.; Zhao, C. S.; Wul, X.; Lu, D. F. Aggregation experiments on fine fly ash particles in a gradient magnetic field. *Chem. Eng. Technol.* **2007**, *30* (8), 1045–1049.

(15) Tao, Z.; Zenghui, W.; Ruichang, Y. Optimization and improvement of $PM_{2.5}$ thermophoretic deposition efficiency in turbulent gas flowing over tube surfaces. *J. Colloid Interface Sci.* **2005**, *289* (1), 36–41.

(16) Wei, F; Zhang, J. Y; Zheng, C. G. Agglomeration rate and action forces between atomized particles of agglomerator and inhaled-particles from coal combustion. *J. Environ. Sci. (China)* **2005**, *17* (2), 335–339.

(17) Durham, M; Bustard, J.; Martin, C.; Baldrey, K.; Starns, T.; Comer, J.; Millar,T.; Lindsey, C. Success with non-traditional flue gas conditioning for hot- and cold-side ESPs. Presented at the *U.S. EPA/DOE/EPRI Combined Power Plant Air Pollutant Control Symposium: The Mega Symposium*, Chicago, IL, Aug 20−23, 2001.

(18) Gillies, G.; Buscher, K.; Preuss, M.; Kappl, M.; Butt, H. J.; Graf, K. Contact angles and wetting behaviour of single micron-sized particles. *J. Phys.: Condens. Matter* **2005**, *17* (9), S445–S464.

(19) Yan, J. P.; Yang., L. J; Shen, X. L. Wettability of $PM_{2.5}$ from combustion. *J. Southeast Univ. (China)* **2006**, *36* (5), 760–764.

(20) Li, H. L; Zhag, J. Y.; Ding, F.; Zheng, C. G. Wettability of fly ash from coal fired power plant. *J. Chem. Ind. Eng. (China)* **2009**, *60* (3), 744–749.

(21) Ulusoy, U.; Yekeler, M.; Hicyilmaz, C. Determination of the shape, morphological and wettability properties of quartz and their correlations. *Miner. Eng.* **2003**, *16* (10), 951–964.

(22) Ralston, J.; Dukhin, S. S.; Mishchuk, N. A. Inertial hydrodynamic particle−bubble interaction in flotation. *Int. J. Miner. Process.* **1999**, *56* (1−4), 207–256.

(23) Dai, Z. F.; Fornasiero, D.; Ralston, J. Particle−bubble attachment in mineral flotation. *J. Colloid Interface Sci.* **1999**, *217* (1), 70–76.

(24) Wu, C.; Peng, X. L.; Li, M.; Wu, G. M. New measuring method of dust wetting agent performances and its application. *J. Nonferrous Met. (China)* **2007**, *17* (5), 830–835.

(25) Chau, T. T.; Bruckard, W. J.; Koh, P. T. L.; Nguyen, A. V. A review of factors that affect contact angle and implications for flotation practice. *Adv. Colloid Interface Sci.* **2009**, *150* (2), 106–115.

(26) Li, H. L.; Zhag, J. Y.; Zhao, Y. C.; Zhang, K.; Zhang, L. Q.; Zheng, C. G. Study on physicochemical characteristic and wetting mechanism of fly ash from coal fired power plant. *J. Eng. Thermophys. (China)* **2009**, *30* (9), 1597–1600.

(27) Simoncic, B.; Roman, V. Wettability of cotton fabric by aqueous solutions of surfactants with different structures. *Colloids Surf.* **2007**, *292* (2−3), 236–245.

(28) Neppolian, B.; Wang, Q.; Jung, H.; Choi, H. Ultrasonic-assisted sol−gel method of preparation of TiO_2 nanoparticles: Characterization, properties and 4-chlorophenol removal application. *Ultrason. Sonochem.* **2008**, *15* (4), 649–658.

(29) Markowski, G. R.; Ensor, D. S.; Hooper, R. G.; Carr, R. C. A submicron aerosol mode in flue gas from a pulverized coal utility boiler. *Environ. Sci. Technol.* **1980**, *14* (11), 1400–1402.

(30) Yekeler, M.; Ulusoy, U.; Hiçyilmaz, C. Effect of particle shape and roughness of talc mineral ground by different mills on the wettability and floatability. *Powder Technol.* **2004**, *140* (1−2), 68–78.

(31) Seames, W. S. An initial study of the fine fragmentation fly ash particle mode generated during pulverized coal combustion. *Fuel Process. Technol.* **2003**, *81* (2), 109–125.

(32) Moreno, N.; Querol, X.; Andrés, J. M.; Stanton, K.; Towler, M.; Nugteren, H.; Janssen-Jurkovicová, M.; Jones, R. Physico-chemical characteristics of European pulverized coal combustion fly ashes. *Fuel* **2005**, *84* (11), 1351–1363.

(33) Medina, A.; Gamero, P.; Querol, X.; Moreno, N.; De León, B.; Almanza, M.; Vargas, G.; Izquierdo, M.; Font, O. Fly ash from a Mexican mineral coal I: Mineralogical and chemical characterization. *J. Hazard. Mater.* **2010**, *181* (1−3), 82–90.

(34) Wang, L.; Cui, Y. S. The application and development of fly ash in China. Presented at the *2007 World of Coal Ash Conference*, Covington, KY, May 7−10, 2007.

(35) Lupu, C.; Jackson, K. L.; Bard, S.; Barron, A. R. Water, acid, and calcium carbonate pretreatment of fly ash: The effect on setting of cement-fly ash mixtures. *Ind. Eng. Chem. Res.* **2007**, *46*, 8018–8025.

(36) Large, D. J.; Kelly, S.; Spiro, B.; Tian, L.; Shao, L.; Finkelman, R.; Zhang, M.; Somerfield, C.; Plint, S.; Ali, Y.; Zhou, Y. Silica-volatile interaction and the geological cause of the xuan wei lung cancer epidemic. *Environ. Sci. Technol.* **2009**, *43* (23), 9016–9021.

(37) Dai, S.; Zhao, L.; Peng, S.; Chou, C. L.; Wang, X.; Zhang, Y.; Li, D.; Sun, Y. Abundances and distribution of minerals and elements in high-alumina coal fly ash from the Jungar Power Plant, Inner Mongolia, China. *Int. J. Coal Geol.* **2010**, *81* (4), 320–332.

(38) Grzeszczyk, S.; Lipowski, G. Effect of content and particle size distribution of high-calcium fly ash on the rheological properties of cement pastes. *Cem. Concr. Res.* **1997**, *27* (6), 907–916.

(39) Zhao, Y. C. Formation mechanism and interaction of fly ash and trace elements during coal combustion. *Ph.D. Thesis*, Huazhong University of Science and Technology, Wuhan, China, 2008.

(40) ASTM standard specification for coal fly ash and raw or calcined natural pozzolan for use in concrete (C618-05). In *Annual Book of ASTM Standards*; ASTM International: West Conshohocken, PA, 2005.

(41) Chau, T. T. A review of techniques for measurement of contact angles and their applicability on mineral surfaces. *Miner. Eng.* **2009**, *22* (3), 213–219.

(42) Koukouzas, N. K.; Zeng, R.; Perdikatsis, V.; Xu, W.; Kakaras, E. K. Mineralogy and geochemistry of Greek and Chinese coal fly ash. *Fuel* **2006**, *85* (16), 2301–2309.

(43) Tian, L. Coal combustion emissions and lung cancer in Xuan Wei, China. *Ph.D. Thesis*, University of California, Berkeley, CA, 2005.

(44) Zdziennicka, A.; Janczuk, B. Effect of anionic surfactant and short-chain alcohol mixtures on adsorption at quartz/water and water/air interfaces and the wettability of quartz. *J. Colloid Interface Sci.* **2011**, *354* (1), 396–404.

(45) Vassilev, S. V.; Yossifova, M. G.; Vassileva, C. G. Mineralogy and geochemistry of Bobov Dol coals, Bulgaria. *Int. J. Coal Geol.* **1994**, *26* (3−4), 185–213.

(46) Ward, C. R. Analysis and significance of mineral matter in coal seams. *Int. J. Coal Geol.* **2002**, *50* (1−4), 135–168.

(47) Zhao, Y. C.; Zhang, J. Y.; Tian, C.; Li, H. L; Shao, X. Y; Zheng, C. G. Mineralogy and chemical composition of high-calcium fly ashes and density fractions from a coal-fired power plant in China. *Energy Fuels* **2010**, *24* (2), 834–843.

(48) Zhao, Y. C.; Zhang, J. Y.; Sun, J. M.; Bai, X. F.; Zheng, C. G. Mineralogy, chemical composition, and microstructure of ferrospheres in fly ashes from coal combustion. *Energy Fuels* **2006**, *20* (4), 1490–1497.

(49) Iveson, S. M.; Holt, S.; Biggs, S. Advancing contact angle of iron ores as a function of their hematite and goethite content: Implications for pelletising and sintering. *Int. J. Miner. Process.* **2004**, *74* (1−4), 281–287.